

# Size Focusing of Nanoparticles by Thermodynamic Control through Ligand Interactions. Molecular Clusters Compared with Nanoparticles of Metals

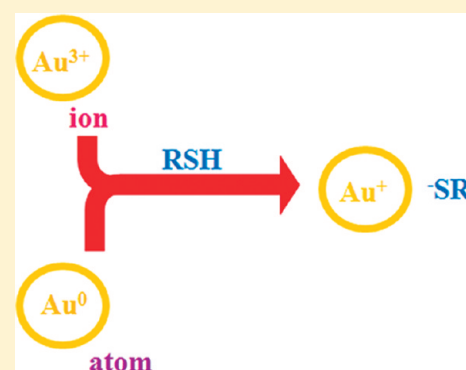
Deepa Jose,<sup>†</sup> John E. Matthiesen,<sup>†,‡</sup> Christopher Parsons,<sup>†,§</sup> Christopher M. Sorensen,<sup>‡</sup> and Kenneth J. Klabunde<sup>\*,†</sup>

<sup>†</sup>Department of Chemistry and <sup>‡</sup>Department of Physics, Kansas State University, Manhattan, Kansas 66506, United States

<sup>‡</sup>Wartburg College, Waverly, Iowa 50677, United States

<sup>§</sup>Department of Chemistry, University of Georgia, Athens, Georgia 30602, United States

**ABSTRACT:** Ligand-capped metal entities come in two sizes, (1) molecular clusters of 10–200 metal atoms and (2) nanoparticles of 2000–10000 metal atoms. In numerous cases, certain “magic sizes” have been found to be most accessible and stable, clusters of 25, 38, 55, and 102 atoms and nanoparticles of 3500–5000 atoms or 4–5 nm. The most familiar and studied system is that of gold (metal) and thiol (ligand). Herein, the methods of synthesis of these gold clusters versus gold nanoparticles are carefully compared. In the cluster case, an important intermediate is the  $(\text{Au}^+\text{SR}^-)_n$  polymer, which is not the case in the synthesis of nanoparticles either from metal (vapor) atoms or metal ions. Also, it is shown that thiol can act as both a reductant ( $\text{Au}^{3+} \rightarrow \text{Au}^+$ ) and as an oxidant ( $\text{Au}^0 \rightarrow \text{Au}^+$ ). The thermodynamic forces responsible for the favored formation of certain size clusters and nanoparticles are discussed.



In what has become a large and vigorous research area, that of ligand-capped metal nanoparticles, a tendency toward certain sizes has been observed by many workers.<sup>1–12</sup> Gold has been studied most extensively, and it has been interesting to observe that the results can be separated into two categories, (1) small nanocrystals, better termed clusters of gold atoms, such as  $\text{Au}_{24}$ ,<sup>13</sup>  $\text{Au}_{25}$ ,<sup>14–18</sup>  $\text{Au}_{38}$ ,<sup>11,19</sup>  $\text{Au}_{102}$ ,<sup>20</sup>  $\text{Au}_{130}$ ,<sup>21</sup>  $\text{Au}_{144}$ ,<sup>22</sup>  $\text{Au}_{225}$ ,<sup>23</sup> and a few others and (2) gold nanoparticles of 3–5 nm (1000–4000 atoms)<sup>1–5</sup> and sometimes 9–10 nm.<sup>24</sup> For both categories, it has been shown that there are clearly numerous examples of size focusing under apparent thermodynamic control. In the case of the “larger” particles, this has been called digestive ripening, although with the clusters, it has been called size focusing.

A fair question is, what features of the synthetic methods employed caused this thermodynamic control? Also, why are these vastly different sizes obtained? The ligands employed are certainly important. For example, excess dodecylthiol with gold nanoparticles under reflux in toluene led to monodisperse  $4.5 \pm 0.4$  nm particles,<sup>4</sup> and variation in alkyl chain length led to only minor changes in the sizes achieved.<sup>25</sup> On the other hand, dodecylamine led to narrow size distribution with  $8.6 \pm 1.3$  nm size.<sup>24</sup> Interestingly, these results were found with two quite different synthetic approaches, metal-vapor-derived nanoparticles<sup>4</sup> where only zerovalent particles were present and inverse micelle-stabilized gold ions reduced by sodium borohydride eventually leading to zerovalent particles.<sup>26</sup> It should be noted that the digestive ripening step was carried out in refluxing organic solvents, usually toluene. When a similar approach was carried

out in water, using water-soluble thiol ligands, digestive ripening still occurred, but the resultant nanoparticles were slightly smaller ( $4.2 \pm 0.5$  nm).<sup>27</sup>

For the gold cluster work, the synthetic approaches are quite different and usually include a two-step reduction of  $\text{Au}(\text{III})$  with polymeric  $\text{Au}(\text{I})\text{-SR}$  formed as an intermediate.<sup>15</sup> Also, the thiols studied in the gold thiol work were of different structures. The most commonly used was 2-phenylethanethiol [ $\text{C}_6\text{H}_5\text{CH}_2\text{-CH}_2\text{SH}$ ] or water-soluble thiols such as glutathione.<sup>10</sup> In comparison, in the nanoparticles work, usually long chained alkyl thiols were employed such as straight-chained dodecylthiol [ $\text{C}_{12}\text{H}_{25}\text{SH}$ ]. Also, different thiol concentrations employed could play a role because in the cluster work, very high concentrations are generally used as compared to nanoparticle work.

A comparative study was needed, which will be discussed now.

**Solvated Metal Atom Dispersion (SMAD).** The metal vapor method employed the solvated metal atom dispersion (SMAD) process.<sup>4</sup> Metal vapor (atoms) is trapped in frozen solvent at 77 K, and upon warming, the atoms migrate to find other atoms, and nanoparticles are thus formed. Ultimate size depends on the solvent employed, amount used, and polarity. Solvents such as acetone, butanone, or tetrahydrofuran (THF) allow stable colloids to form with gold, which are red in color, show an absorption in the UV–vis representative of a plasmon

Received: December 13, 2011

Accepted: March 8, 2012

Published: March 8, 2012

resonance (520 nm), and are, by TEM bright field imaging, 2–8 nm in size when butanone is used as a solvent (see Scheme 1 and Figure 1a).

**Scheme 1. Metal Vapor Method (SMAD) for Preparing Nanoparticles of Gold in a Weakly Coordinating Solvent, Followed by Treatment with Thiols**

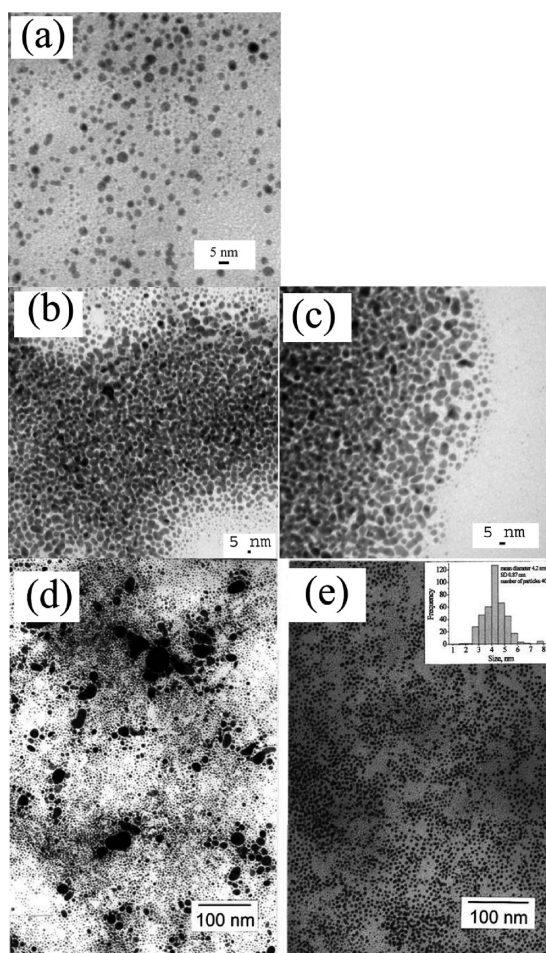
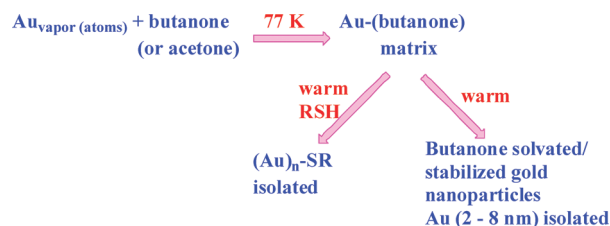


**Figure 1.** TEM images of SMAD for (a) isolated gold–butanone colloid and (b) gold-2-phenylethanethiol immediately after isolation and (c) after digestive ripening in toluene; (d) gold-dodecylthiol immediately after isolation and (e) after digestive ripening. (Inset) Histogram showing particle size distribution [(d) and (e) from ref 4].

When the gold–butanone cold matrix was allowed to melt down and mix with a thiol ligand, immediately, the weakly solvating butanone was replaced by R-SH. Two thiols were compared, dodecylthiol (DDT) and 2-phenylethanethiol (PET). The colloids formed were brown (DDT) and yellow–brown (PET). Both exhibited featureless UV–vis spectra with decreasing absorption with increasing wavelength. However, the two thiols did behave differently over time, the DDT

colloid being very stable while the PET colloid was not, and a precipitate formed that resisted redissolution. This precipitate was probably a Au(I)-thiolate polymer (see later discussion).

**Digestive Ripening.** A direct comparison of DDT and PET in toluene solvent was carried out. In these experiments, DDT or PET was placed in the bottom of the reactor, vacuum and liquid nitrogen cooling was applied, and toluene vapor was deposited on the reactor walls. Then, the cooling dewar was removed and toluene allowed to melt and mix with the DDT (or PET). Then, cooling was again applied, and the vapors of acetone (or butanone) were codeposited with gold vapor. Upon completion, the acetone–gold matrix was allowed to melt, and atom accretion began as the melt moved down and mixed with the toluene–DDT (or PET) solution.

**Gold–Acetone–Toluene–2-Phenylethanethiol Colloid.** The as-prepared gold–acetone–toluene–2-phenylethanethiol colloid was brownish red in color, and the UV–visible spectrum showed a shoulder at around 500 nm. The TEM bright field images of the as-prepared sample showed a mixture of particles, isolated spherical particles of size varying from 2 to 40 nm and necked particles of no definite geometry (Figure 1b). The digestive ripening of the as-prepared sample for 1.5 h in toluene after the removal of acetone did not show any change in the color (brownish red). The UV–visible spectrum did not change. The TEM bright field image of the digestively ripened sample showed a network of necked particles along with a few isolated spherical particles (Figure 1c).

**Gold–Acetone–Toluene–Dodecylthiol Colloid.**<sup>4</sup> The as-prepared gold–acetone–toluene–dodecylthiol colloid was dark brown in color with particles of no definite geometrical shapes and size varying from 5 to 40 nm (Figure 1d). The UV–visible spectrum of the as-prepared sample was very broad, which is consistent with the TEM results. The digestive ripening of the as-prepared dodecylthiol-capped gold colloid in toluene after removal of the initial weak capping agent, acetone, gave great improvement in the particle size distribution. The average particle diameter was found to be  $4.5 \pm 0.4$  nm after digestive ripening for 1.5 h (Figure 1e). Also, the UV–visible spectrum of the digestively ripened sample became narrow with an absorption maximum at around 513 nm.<sup>4</sup>

**Inverse Micelle Method.**<sup>28</sup> To repeat, the main interest was in comparing DDT and PET. In the inverse micelle method, gold salts are reduced in the presence of a surfactant in an organic solvent containing small amounts of water.<sup>28</sup> Usually, the reducing agent is  $\text{NaBH}_4$ . When didodecyldimethylammonium bromide (DDAB) was used as the surfactant and  $\text{NaBH}_4$  as a reducing agent, upon addition of DDT, the orange solution turned purple–red immediately. However, when PET was added, a dark blue color resulted. When the colloidal gold particles were isolated by precipitation with ethanol, washed, and dried, the DDT particles were readily soluble in toluene. However, the PET particles were quite insoluble, and only by using sonication could they be resuspended. TEM studies (Figure 2a) showed in the case of PET, agglomerated masses of very small particles. Similar results were observed when THF was used as the solvent in place of toluene. Thus, to summarize, nanoparticles formed with DDT followed by digestive ripening always yielded spherical quasi-monodisperse particles in the 5 nm size range (4.6–5.5 nm). This was true even with comparing several preparations and even different solvents (toluene or THF). However, digestive ripening using PET led to a network of small particles, more polymeric in nature (Figure 2b).



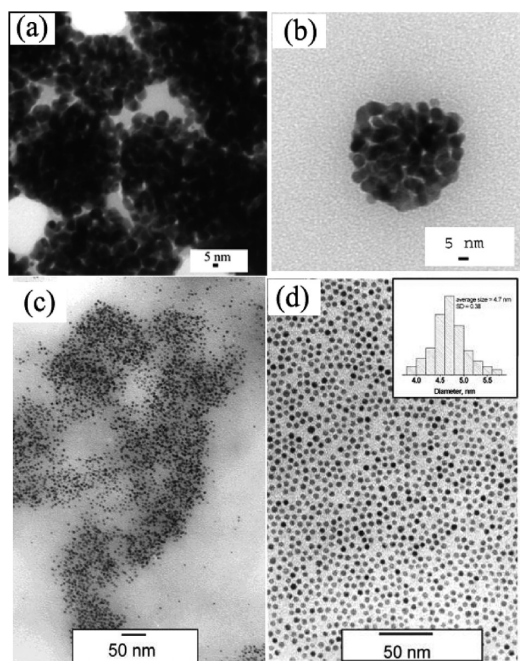
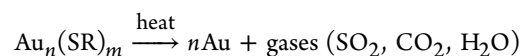
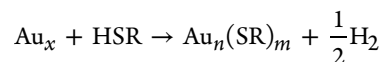


**Figure 2.** Inverse micelle TEM bright field images of Au–PET and Au–DDT colloids (a) PET before digestive ripening, (b) PET after digestive ripening, (c) DDT before digestive ripening, and (d) DDT after digestive ripening. (Inset) Histogram showing particle size distribution [(c) and (d) from ref 25].

At this point, it is useful to describe the differences between DDT and PET under the same experimental conditions. In the case of DDT, the tendency is toward growing 5 nm gold particles, and these are honed to near-monodispersity by digestive ripening (Figure 2c and d). However, in the case of PET, the gold particles formed by the SMAD method or the inverse micelle method tend toward very small particles that strongly aggregate. That is, under both experimental conditions, SMAD and inverse micelle, when PET is used, the product formed is aggregated networks of necked particles. Moreover, a Au(I)-thiolate polymer was formed from the as-prepared Au–butanone–PET SMAD colloid after storing under argon for several days.

Above, the two categories of gold nanoparticle research were brought up, (1) very small nanoparticles where Au clusters of 25, 38, 105, and 225 atoms and others have been isolated as thiolate complexes, either neutral or negatively charged overall, and (2) the large class of gold–thiolate particles around 5 nm, or usually about  $\text{Au}_{3800}(\text{SR})_{365}$ . In the latter case of the 5 nm particles, because no X-ray crystal structures have been possible to obtain, the evidence for thiolate  $[\text{RS}^-]$  versus  $\text{RSH}$  as the capping ligand has not been as clear.<sup>29</sup> However, on the basis of the recent evidence of Creutz and co-workers and others,<sup>30</sup> when surfactant-stabilized gold nanoparticles were allowed to react with thiols, a substantial portion, though not quantitative, of hydrogen gas was released. Inspired by the Creutz work and by years of uncertainty of what actually happens to the hydrogen in gold–thiol reactions, a series of SMAD experiments were carried out. Here, weakly solvated gold nanoparticles (acetone solvent) were allowed to contact dodecylthiol, and hydrogen gas was evolved upon warming up to room temperature. Control experiments with pure acetone did not show hydrogen gas evolution (unpublished results).

In the case of DDT, the amount of hydrogen evolved was 15  $\mu\text{mol}$  and 230  $\mu\text{mol}$  of gold was used, while in the case of PET, 31  $\mu\text{mol}$  of  $\text{H}_2$  was evolved and 456  $\mu\text{mol}$  of gold was used. In another set of experiments, the isolated, purified gold–thiol nanoparticles were analyzed by thermogravimetric analysis (TGA) by heating in air, and the thiol/thiolate was oxidized away, leaving only gold. The results for DDT were 0.75  $\mu\text{mol}$  of thiolate versus 6.2  $\mu\text{mol}$  of gold, and those for PET were 3.2  $\mu\text{mol}$  of thiolate versus 25  $\mu\text{mol}$  of gold.



Comparing these experimental approaches indicated that the moles of hydrogen gas produced were about equal to the moles of thiolate produced within 7%. These data also indicated that there are eight times as many atoms of gold as thiolate molecules; by  $\text{H}_2$  production,  $\text{Au}/\text{H} = 7.6$ , and by TGA,  $\text{Au}/\text{SR} = 8.2$ . The same experiments with PET yielded essentially the same results with respect to hydrogen/gold and thiolate/gold. The ratios were  $\text{Au}/\text{H} = 7.4$  and  $\text{Au}/\text{SR} = 7.7$ . It can be concluded that at room temperature, both DDT and PET react with weakly solvated gold nanoparticles to form gold–thiolate structures plus hydrogen gas.

**It can be concluded that at room temperature, both DDT and PET react with weakly solvated gold nanoparticles to form gold–thiolate structures plus hydrogen gas.**

The TEM results show that SMAD gold–acetone or gold–butanone colloids before the addition of the thiols range from 2–8 nm. These  $\text{Au}/\text{SR}$  ratios can be used to estimate the gold nanoparticle size. We assume spherical particles of gold with a bulk density of 19.3  $\text{g}/\text{cm}^3$ . We take the thiol to occupy a surface area of 0.215  $\text{nm}^2$ .<sup>31</sup> Then, one can show that the total number of gold atoms in the nanoparticle,  $N(\text{Au})$ , and the total number of thiol ligands on the surface of the nanoparticles,  $N(\text{SR})$ , are given by  $N(\text{Au}) = 31d^3$  and  $N(\text{SR}) = 14.67d^2$ , where  $d$  is the particle diameter in nanometers. The  $\text{Au}/\text{SR}$  ratio is identically equal to  $N(\text{Au})/N(\text{SR})$ . Then, with the above equation, one finds  $d = 0.47 \text{ Au}/\text{SR}$ . Above, we found  $\text{Au}/\text{SR} \approx 8$  to imply, by the above equation,  $d \approx 4 \text{ nm}$ . This is quite consistent with TEM observation of the particles that show sizes ranging from 2 to 8 nm.

The main conclusion, however, is that these experiments yield gold–thiolate structures, not gold–thiol.

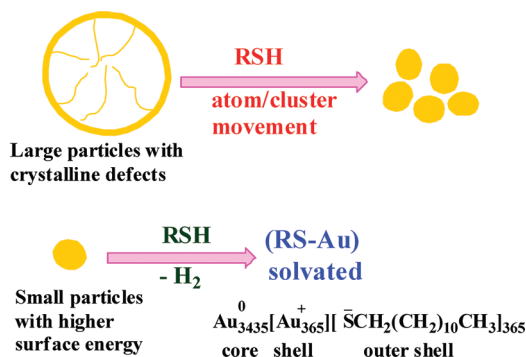
Other zerovalent metal particles readily undergo oxidation by thiol to form thiolates, for example, Pd and Cu.<sup>32–35</sup> However, Au is clearly a borderline case.

**Gold Size Sensitivity to Thiol Attack.** Millimeter size pieces of bulk gold do not react with thiols in any refluxing solvent that has been used for digestive ripening, such as toluene, butanone, tert-butyltoluene, or diphenylether (unpublished results). However, nanoparticle gold does react, but only on the surface. Thus,  $\text{Au}_{3800}$  is a stable entity with 365 thiolates where the thiolate is  $\text{CH}_3(\text{CH}_2)_{10}\text{CH}_2\text{S}^-$ .<sup>36</sup>

It is proposed herein that the surface energy of a 4–5 nm particle is high enough to allow an oxidation reaction with thiol, but only a surface reaction. Smaller particles would have a higher surface energy and thus could be more fully consumed by the thiol  $\rightarrow$  thiolate + hydrogen process.

Digestive ripening results imply that both smaller and larger nanoparticles are modified until one preferred size is attained, about 5 nm. Smaller particles would be more reactive, and under digestive ripening conditions, gold atoms or clusters could be “dissolved” by thiols/thiolates and redispersed on larger particles, similar to Ostwald ripening. Larger nanoparticles would be slightly less reactive and perhaps less subject to the thiol  $\rightarrow$  thiolate + hydrogen process but are subject to thiol–gold atom/cluster solvation and transport. Thereby, gold atoms or clusters could be transported to other particles. This seems especially likely if crystalline defects in the larger particles are present (Scheme 2).

**Scheme 2. Illustration of Thiol Attack on Larger, Polycrystalline Gold Nanoparticles<sup>39</sup>**



Indeed, this type of movement was clearly shown to be possible when thiolated 5 nm particles of Au and 5 nm particles of Ag were digestively ripened together to form alloy particles of the same size!<sup>37,38</sup> Thus, a thermodynamic equilibration could be set up and would be sensitive to the nanoparticle's size. These data suggest that 5 nm is a critical size, possessing the optimum surface energy to allow a shell of Au-SR to form and thus protect the core of Au<sup>0</sup> from further reaction. Of course, this concept is perhaps acceptable for less reactive thiols such as dodecylthiol and not with more reactive thiols. Also, other head groups such as amines have been found to lead to larger digestively ripened particles, and clearly, other chemical forces are involved. These delicate thermodynamic equilibria can be affected by ligand head group size and reactivity and metal nanoparticle size.

Next, the category of small clusters is considered. It would appear that a molecular intermediate such as the Au(I)-SR unit is involved. More reactive thiols would favor the formation of such species from zerovalent gold clusters. Furthermore, evidence presented above supports the idea of higher reactivity of PET versus alkyl thiols. Now, considering the second step in synthesizing small gold clusters, the polymer Au(I)-SR (or written formally as Au<sup>+</sup>SR<sup>-</sup>) is exposed to a reducing agent such as NaBH<sub>4</sub>. Upon encountering this reducing agent, Au<sup>+</sup>SR<sup>-</sup> species would tend to form Au<sup>0</sup>SR<sup>-</sup> and thus could build its core up to gold clusters. For example, the most well-known system, Au<sub>25</sub>(SR)<sub>18</sub>, is perhaps better depicted as 7Au<sup>0</sup>, or Au<sub>7</sub>(Au-SR)<sub>18</sub>.

Therefore, if thiols are reactive enough and conditions (temperature, solvent) are vigorous enough, even nanogold zerovalent species could be attacked by thiol repeatedly until

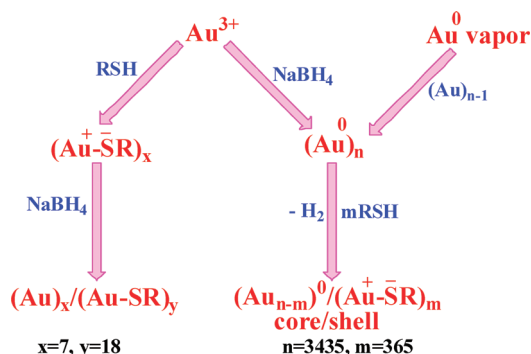
essentially all gold atoms are oxidized. Then, under reducing conditions (NaBH<sub>4</sub> or another reducing agent) and mild temperature, small gold clusters could form, and “buildup” could take place. Along the way, some slightly more stable clusters could be favored, such as Au<sub>25</sub>, Au<sub>38</sub>, Au<sub>105</sub>, or Au<sub>225</sub>, due to the electronic structure or closed shells or other unique features.

**If thiols are reactive enough and conditions (temperature, solvent) are vigorous enough, even nanogold zerovalent species could be attacked by thiol repeatedly until essentially all gold atoms are oxidized.**

Coming back to the larger zerovalent nanoparticles, they would be less reactive than the very small zerovalent clusters. However, under the right conditions, surfaces could be oxidized by thiol. Particle collisions taking place at elevated temperatures of solvent could cause material transfers. Au atoms/clusters or Au<sup>+</sup>SR<sup>-</sup> partners or clusters must be somewhat mobil, which would be assisted by the presence of excess thiol. In support of this idea, it has been found that concentration of nanoparticle gold is important in order to achieve satisfactory digestive ripening results.<sup>38</sup>

Scheme 3 attempts to clarify the possible reaction sequences, and Scheme 4 shows balanced equations including side reactions for the three synthetic methods discussed herein.

**Scheme 3. Possible Reaction Sequence<sup>a</sup>**



<sup>a</sup>If gold nanoparticles are formed in one step followed by thiol treatment, larger (5 nm) core/shell Au/Au-SR particles can be formed. If Au-SR polymer is formed first, followed by thiol treatment, much smaller Au/Au-SR molecules can be formed.

Thiols react with Au(III) to produce Au(I)-SR polymer. Treatment of this thiol polymer with NaBH<sub>4</sub> causes reduction of some Au(I) to Au(0), but Au(I)-SR serves to cap and protect particularly stable, very small gold cores. In this reaction scheme, Au(III) is reduced by thiol to form the Au(I)-SR thiolate polymer.

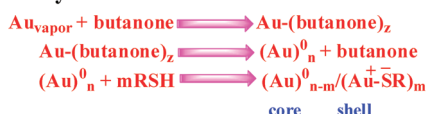
On the other hand, both the SMAD method and inverse micelle method lead to Au atoms that rapidly aggregate to form Au(0) nanoparticles. Thiol reacts with these zerovalent particles to form surface Au(I)-SR capping structures. In this reaction scheme, Au(0) is oxidized by thiol, but only surface gold atoms are attacked. Gold particle size has an influence on the extent of reactivity with thiols. Certain thiols are more reactive in this

#### Scheme 4. Likely Reactions Involved in the Murray et al. Synthesis,<sup>15</sup> the SMAD Synthesis, and the Inverse Micelle Synthesis

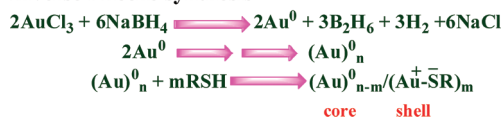
##### Murray et al. synthesis of gold clusters



##### SMAD synthesis



##### Inverse Micelle synthesis



way, and PET is more reactive than DDT (at low temperature, both DDT and PET react with surface gold atoms to quickly evolve  $\text{H}_2$ ; however, PET reacts with butanone-stabilized gold particles to form  $\text{Au}^+\text{SR}^-$  polymer, but DDT does not). This area of size-dependent chemistry of nanoparticles, especially nanoparticle surfaces, controlled by thermodynamics, points toward a “gold mine” of new discoveries. It is likely that many nanomaterials would exhibit such selectivities. This becomes a chemist’s dream because the choice of nanomaterial, ligand, solvent, and temperature can all be used for control. Also, further understanding of how to achieve molecular clusters or monodisperse nanoparticles has been gained.

## AUTHOR INFORMATION

### Corresponding Author

\*Phone: 785-532-6849. E-mail: kenjk@ksu.edu. Fax: 785-532-6666.

### Notes

The authors declare no competing financial interest.

### Biographies

**Deepa Jose** received her Ph.D. in Materials Science from the Indian Institute of Science, Bangalore, India, in 2009. She joined Prof. Klabunde’s group at Kansas State University as a postdoctoral research associate in 2011. Her current research work focuses on the digestive ripening and ligand shell modification of thiol-capped gold nanoparticles.

**John E. Matthiesen** is a fourth year undergraduate student at Wartburg College. He worked with Prof. Klabunde for a NSF REU program in the summer of 2011. His research was mainly focused on finding out the fate of a sulfur-bound hydrogen atom during the interaction of gold nanoparticles with thiols.

**Christopher Parsons** is a third year B.S./M.S. student in chemistry at the University of Georgia. He worked with Prof. Klabunde in the summer of 2011 for a NSF REU program. Currently, he researches in the Marcus D. Lay nanomaterials lab at the University of Georgia.

**Christopher M. Sorensen** is the Cortelyou–Rust University Distinguished Professor at Kansas State University in Physics and

Chemistry (Adjunct). He earned B.S. and Ph.D. degrees at the Universities of Nebraska and Colorado, respectively. His current research focuses on nanoparticle physical chemistry and light scattering. In 2007, he was named the National Professor of the Year for Doctoral and Research Universities by the CASE/Carnegie Foundation for the Advancement of Teaching.

**Kenneth J. Klabunde** received a B.A. degree from Augustana College and a Ph.D. from the University of Iowa in 1969. In 1988, he was appointed as University Distinguished Professor. He is the founder of Nanoscale Corporation, has published numerous papers and written several books in nanoparticles chemistry, and holds over 20 patents. He has won the ACS Midwest Award, University of Iowa alumni award, and Popular Mechanics Magazine Breakthrough Invention Award (for a nanopowder that destroys chemical warfare agents). <http://www.ksu.edu/chem/people/faculty/klabunde.html>

## ACKNOWLEDGMENTS

We are grateful to the Department of Energy (Basic Energy Sciences GOCH 001897) for funding. Also, J.E.M. and C.P. thank the National Science Foundation for summer REU support.

## REFERENCES

- (1) Lin, X. M.; Sorensen, C. M.; Klabunde, K. J. Digestive Ripening, Nanophase Segregation and Superlattice Formation in Gold Nanocrystal Colloids. *J. Nanopart. Res.* **2000**, *2*, 157–164.
- (2) (a) Klabunde, K. J.; Sorensen, C. M.; Stoeva, S. I.; Prasad, B. L. V.; Smetana, A. B.; Lin, X. M. Digestive Ripening, or ‘Nanomachining,’ to Achieve Nanocrystal Size Control, (invited book Chapter). In *Metal Nanoclusters in Catalysis and Materials Science: The Issue of Size Control, Part II Methodologies*; Corrain, C., Schmid, G., Toshima, N., Eds.; Elsevier Science: Amsterdam, The Netherlands, 2008; Chapter 11, pp 233–252. (b) Park, J.; Joo, J.; Kwon, S. G.; Jang, Y.; Hyeon, T. Synthesis of Monodisperse Spherical Nanocrystals. *Angew. Chem., Int. Ed.* **2007**, *46*, 4630–4660. (c) Sidhaye, D. S.; Prasad, B. L. V. Many Manifestations of Digestive Ripening: Monodispersity, Superlattices and Nanomachining. *New J. Chem.* **2011**, *35*, 755–763.
- (3) Prasad, B. L. V.; Sorensen, C. M.; Klabunde, K. J. Gold Nanoparticle Superlattices. *Chem. Soc. Rev.* **2008**, *37*, 1871–1883.
- (4) Stoeva, S.; Klabunde, K. J.; Sorensen, C. M.; Dragieva, I. Gram-Scale Synthesis of Monodisperse Gold Colloids by the Solvated Metal Atom Dispersion Method and Digestive Ripening and Their Organization into Two- and Three-Dimensional Structures. *J. Am. Chem. Soc.* **2002**, *124*, 2305–2311.
- (5) Lin, X. M.; Jaeger, H. M.; Sorensen, C. M.; Klabunde, K. J. Formation of Long-Range-Ordered Nanocrystal Superlattices on Silicon Nitride Surfaces. *J. Phys. Chem. B* **2001**, *105*, 3353–3357.
- (6) Kalidindi, S. B.; Jagirdar, B. R. Highly Monodisperse Colloidal Magnesium Nanoparticles by Room Temperature Digestive Ripening. *Inorg. Chem.* **2009**, *48*, 4524–4529.
- (7) Barngrover, B. M.; Aikens, C. M. Electron and Hydride Addition to Gold(I) Thiolate Oligomers: Implications for Gold-Thiolate Nanoparticle Growth Mechanisms. *J. Phys. Chem. Lett.* **2011**, *2*, 990–994.
- (8) Qian, H.; Zhu, M.; Andersen, U. N.; Jin, R. Facile, Large-Scale Synthesis of Dodecanethiol-Stabilized  $\text{Au}_{38}$  Clusters. *J. Phys. Chem. A* **2009**, *113*, 4281–4284.
- (9) (a) Wu, Z.; MacDonald, M. A.; Chen, J.; Zhang, P.; Jin, R. Kinetic Control and Thermodynamic Selection in the Synthesis of Atomically Precise Gold Nanoclusters. *J. Am. Chem. Soc.* **2011**, *133*, 9670–9673. (b) Chaki, N. K.; Negishi, Y.; Tsunoyama, H.; Shichibu, Y.; Tsukuda, T. Ubiquitous 8 and 29 kDa Gold: Alkanethiolate Cluster Compounds: Mass-Spectrometric Determination of Molecular Formulas and Structural Implications. *J. Am. Chem. Soc.* **2008**, *130*, 8608–8610.



- (10) Wu, Z.; Chen, J.; Jin, R. One-Pot Synthesis of  $\text{Au}_{25}(\text{SG})_{18}$  2- and 4-nm Gold Nanoparticles and Comparison of Their Size-Dependent Properties. *Adv. Funct. Mater.* **2011**, *21*, 177–183.
- (11) Qian, H.; Zhu, Y.; Jin, R. Size-Focusing Synthesis, Optical and Electrochemical Properties of Monodisperse  $\text{Au}_{38}(\text{SC}_2\text{H}_4\text{Ph})_{24}$  Nanoclusters. *ACS Nano* **2009**, *3*, 3795–3803.
- (12) Qian, H.; Jin, R. Controlling Nanoparticles with Atomic Precision: The Case of  $\text{Au}_{144}(\text{SCH}_2\text{CH}_2\text{Ph})_{60}$ . *Nano Lett.* **2009**, *9*, 4083–4087.
- (13) Zhu, M.; Qian, H.; Jin, R. Thiolate-Protected  $\text{Au}_{24}(\text{SC}_2\text{H}_4\text{Ph})_{20}$  Nanoclusters: Superatoms or Not? *J. Phys. Chem. Lett.* **2010**, *1*, 1003–1007.
- (14) Akola, J.; Walter, M.; Whetten, R. L.; Häkkinen, H.; Grönbeck, H. On the Structure of Thiolate-Protected  $\text{Au}_{25}$ . *J. Am. Chem. Soc.* **2008**, *130*, 3756–3757.
- (15) Parker, J. F.; Weaver, J. E. F.; McCallum, F.; Fields-Zinna, C. A.; Murray, R. W. Synthesis of Monodisperse  $[\text{Au}_{25}(\text{SR})_{18}]^{-}[\text{Oct}_4\text{N}^{+}]$  Nanoparticles, with Some Mechanistic Observations. *Langmuir* **2010**, *26*, 13650–13654.
- (16) Wu, Z.; Suhan, J.; Jin, R. One-Pot Synthesis of Atomically Monodisperse, Thiol-Functionalized  $\text{Au}_{25}$  Nanoclusters. *J. Mater. Chem.* **2009**, *19*, 622–626.
- (17) Zhu, M.; Chan, G.; Qian, H.; Jin, R. Unexpected Reactivity of  $\text{Au}_{25}(\text{SCH}_2\text{CH}_2\text{Ph})_{18}$  Nanoclusters with Salts. *Nanoscale* **2011**, *3*, 1703–1707.
- (18) Parker, J. F.; Kacprzak, K. A.; Lopez-Acevedo, O.; Häkkinen, H.; Murray, R. W. Experimental and Density Functional Theory Analysis of Serial Introductions of Electron-Withdrawing Ligands into the Ligand Shell of a Thiolate-Protected  $\text{Au}_{25}$  Nanoparticle. *J. Phys. Chem. C* **2010**, *114*, 8276–8281.
- (19) Donkers, R. L.; Lee, D.; Murray, R. W. Synthesis and Isolation of the Molecule-like Cluster  $\text{Au}_{38}(\text{PhCH}_2\text{CH}_2\text{S})_{24}$ . *Langmuir* **2004**, *20*, 1945–1952.
- (20) Levi-Kalishman, Y.; Jadzinsky, P. D.; Kalishman, N.; Tsunoyama, H.; Tsukuda, T.; Bushnell, D. A.; Kornberg, R. D. Synthesis and Characterization of  $\text{Au}_{102}(\text{p-MBA})_{44}$  Nanoparticles. *J. Am. Chem. Soc.* **2011**, *133*, 2976–2982.
- (21) Tang, Z.; Robinson, D. A.; Bokossa, N.; Xu, B.; Wang, S.; Wang, G. Mixed Dithiolate Durene-DT and Monothiolate Phenylethanethiolate Protected  $\text{Au}_{130}$  Nanoparticles with Discrete Core and Core-Ligand Energy States. *J. Am. Chem. Soc.* **2011**, *133*, 16037–16044.
- (22) Qian, H.; Jin, R. Ambient Synthesis of  $\text{Au}_{144}(\text{SR})_{60}$  Nanoclusters in Methanol. *Chem. Mater.* **2011**, *23*, 2209–2217.
- (23) Wolfe, R. L.; Murray, R. W. Analytical Evidence for the Monolayer-Protected Cluster  $\text{Au}_{225}[(\text{S}(\text{CH}_2)\text{CH}_3)]_{75}$ . *Anal. Chem.* **2006**, *78*, 1167–1173.
- (24) Prasad, B. L. V.; Stoeva, S. I.; Sorensen, C. M.; Klabunde, K. J. Digestive-Ripening Agents for Gold Nanoparticles: Alternatives to Thiols. *Chem. Mater.* **2003**, *15*, 935–942.
- (25) Prasad, B. L. V.; Stoeva, S. I.; Sorensen, C. M.; Klabunde, K. J. Digestive Ripening of Thiolated Gold Nanoparticles: The Effect of Alkyl Chain Length. *Langmuir* **2002**, *18*, 7515–7520.
- (26) Stoeva, S. I.; Prasad, B. L. V.; Uma, S.; Stoimenov, P.; Zaikovski, V.; Sorensen, C. M.; Klabunde, K. J. Face-Centered Cubic and Hexagonal Close-Packed Nanocrystal Superlattices of Gold Nanoparticles Prepared by Different Methods. *J. Phys. Chem. B* **2003**, *107*, 7441–7448.
- (27) Stoeva, S. I.; Smetana, A. B.; Sorensen, C. M.; Klabunde, K. J. Gram-Scale Synthesis of Aqueous Gold Colloids Stabilized by Various Ligands. *J. Colloid Interface Sci.* **2007**, *309*, 94–98.
- (28) Pileni, M. P. Nanocrystal Self-Assemblies: Fabrication and Collective Properties. *J. Phys. Chem. B* **2001**, *105*, 3358–3371.
- (29) Hasan, M.; Bethell, D.; Brust, M. The Fate of Sulfur-Bound Hydrogen on Formation of Self-Assembled Thiol Monolayers on Gold:  $^1\text{H}$  NMR Spectroscopic Evidence from Solutions of Gold Clusters. *J. Am. Chem. Soc.* **2002**, *124*, 1132–1133.
- (30) (a) Petroski, J.; Chou, M.; Creutz, C. The Coordination Chemistry of Gold Surfaces: Formation and Far-Infrared Spectra of Alkanethiolate-Capped Gold Nanoparticles. *J. Organomet. Chem.* **2009**, *694*, 1138–1143. (b) Edinger, K.; Götzhäuser, A.; Demota, K.; Wöll, Ch.; Grunze, M. Formation of Self-Assembled Monolayers of *n*-Alkanethiols on Gold: A Scanning Tunneling Microscopy Study on the Modification of Substrate Morphology. *Langmuir* **1993**, *9*, 4–8. (c) Biener, M. M.; Biener, J.; Friend, C. M. Revisiting the S-Au(111) Interaction: Static or Dynamic? *Langmuir* **2005**, *21*, 1668–1671.
- (31) Poirier, G. E.; Pylant, E. D. The Self-Assembly Mechanism of Alkane Thiols on Au (111). *Science* **1996**, *272*, 1145–1148.
- (32) Yang, Z.; Smetana, A. B.; Sorensen, C. M.; Klabunde, K. J. Synthesis and Characterization of a New Tiara Pd(II) Thiolate Complex —  $[\text{PdSC}_{12}\text{H}_{25}]_6$  and Its Solution-Phase Thermolysis to Prepare Nearly Monodisperse Palladium Sulfide Nanoparticles. *Inorg. Chem.* **2007**, *46*, 2427–2431.
- (33) Yang, Z.; Klabunde, K. J.; Sorensen, C. M. From Monodisperse Sulfurized Palladium Nanoparticles to Tiara Pd(II) Thiolate Clusters: The Influence of Thiol Ligand on the Thermal Treatment of a Pd(II)-Amine System. *J. Phys. Chem. C* **2007**, *111*, 18143–18147.
- (34) Ponce, A. A.; Klabunde, K. J. Chemical and Catalytic Activity of Copper Nanoparticles Prepared Via Metal Vapor Synthesis. *J. Mol. Catal. A: Chem.* **2005**, *225*, 1–6.
- (35) Ponce, A. A.; Smetana, A.; Stoeva, S.; Klabunde, K. J.; Sorensen, C. M. Nanocrystal Superlattices of Copper, Silver and Gold, by Nanomachining. In *Nanostructured and Advanced Materials*; Vaseashta, A., et al., Eds.; Springer: The Netherlands, 2005; pp 309–316.
- (36) Sorensen, C. M. Nanoparticle Solutions. In *Nanoscale Materials in Chemistry: Environmental Applications*; ACS Symposium Series 1045; Erickson, L. E., Koodali, R. J., Richards, R. M., Eds.; 2010; Chapter 3, pp 35–49.
- (37) Smetana, A. B.; Klabunde, K. J.; Sorensen, C. M.; Ponce, A. A.; Mwale, B. Low Temperature Metallic Alloying of Copper and Silver Nanoparticles with Gold Nanoparticles through Digestive Ripening. *J. Phys. Chem. B* **2006**, *110*, 2155–2158.
- (38) Smetana, A. Ph.D thesis, Kansas State University, 2006.
- (39) Stoeva, S. I.; Zaikovski, V.; Prasad, B. L. V.; Stoimenov, P. K.; Sorensen, C. M.; Klabunde, K. J. Reversible Transformations of Gold Nanoparticle Morphology. *Langmuir* **2005**, *21*, 10280–10283.